

Magnetization-induced second harmonic generation from the Ni/Cu interface in multilayers on Cu(001)

Y. Z. Wu,^{1,2} R. Vollmer,^{1,*} H. Regensburger,¹ X.-F. Jin,² and J. Kirschner¹

¹Max-Planck-Institut für Mikrostrukturphysik, Weinberg 2, D-06120 Halle/Saale, Germany

²Surface Physics Laboratory, Fudan University, Shanghai, 200433, People's Republic of China

(Received 6 June 2000; published 22 December 2000)

Ultrathin Ni films in Cu/Ni/Cu(001) bilayers and exchange coupled Ni films in Ni/Cu/Ni/Cu(001) trilayers are investigated by magnetization induced second harmonic generation (MSHG). The results are analyzed in a model of localized nonlinear polarizabilities at the interfaces. We show that antiferromagnetic coupling in the Ni/Cu/Ni trilayers is observable with MSHG due to the presence of quantum well states (QWS's) in the Cu layer. The influence of the QWS's on the SHG from a Ni film in a Cu/Ni/Cu(001) bilayer is weaker compared to the case of Fe or Co bilayers.

DOI: 10.1103/PhysRevB.63.054401

PACS number(s): 75.70.Cn, 78.20.Ls, 42.65.Ky

I. INTRODUCTION

Magnetization-induced second harmonic generation (MSHG) from surfaces and thin films of ferromagnetic materials has been shown in the past to be a very surface and interface sensitive probe.¹ This surface and interface sensitivity comes from the fact, that in materials having a center of inversion second harmonic generation (SHG) is forbidden by symmetry selection rules within the dipole approximation. Compared to the magneto-optical Kerr effect (MOKE) in the linear reflected light, the relative magneto-optical effects in the frequency doubled light like the MSHG asymmetry^{2,3} and Kerr angle⁴ were found to be up to several orders of magnitude larger. Therefore, despite the quite low efficiency of SHG from interfaces, MSHG can be used conveniently to study the magnetic behavior of ultrathin magnetic films and multilayers.

In metallic sandwich structures of 3d-metal films of Co and Fe covered by noble metals like Cu and Au a strong influence of the SH intensity on the thickness of the noble metal cover layer has been observed.⁵⁻⁸ This has been explained within the dipole approximation by a resonance phenomenon between certain thin film states [quantum well states (QWS's)] of the noble metal and *d* states derived from the transition metal.⁸⁻¹⁰ A similar interpretation was made by Ref. 11 for the oscillations of the second harmonic (SH) light generated from Ag/Si(111). Summarizing the current understanding, it is expected, that the SH light in the above mentioned systems is generated mostly at the interfaces, even in the case that QWS's are involved.

In this paper we describe the MSHG from ultrathin Ni/Cu/Ni trilayers on Cu(001), where the two Ni films couple ferromagnetically (FM) or antiferromagnetically (AF), depending on the thickness of the Cu spacer layer. After a short description of the experimental setup in Sec. II we describe a simple model based on local SH generation from multilayers in Sec. III. In Sec. IV A we report on effects of QWS's from a Cu/Ni bilayer on Cu(001) and compare them to that from Cu/Fe and Cu/Co bilayers on the same substrate before we present the experimental results on the Ni/Cu/Ni trilayer in Sec. IV B. After the discussion in Sec. V we conclude in

Sec. VI that in Ni/Cu/Ni trilayers on Cu(001) antiferromagnetic coupling can be detected by MSHG and that within the model presented in Sec. III the presence of QWS is a *necessary* prerequisite for the observability of this coupling.

II. EXPERIMENT

The Ni and the other ferromagnetic (FM) films were deposited onto a Cu(001) single crystal having a miscut of less than 0.2° in an UHV molecular beam epitaxy (MBE) apparatus with a base pressure of less than 4×10^{-11} mbar. The thickness of the FM film was determined by means of medium energy electron diffraction (MEED) oscillations during the growth. The transition metal films were all grown at about 300 K with a growth rate of the order of 1 ML/min. The Cu deposition rate was calibrated by MEED oscillations prior to the growth of the Cu wedge. The experimental uncertainty in the thickness determination was less than 10%.

For the growth of the exchange coupled Ni multilayer structures the Ni films were deposited at $T=293$ K. After the growth of the first Ni film the sample was annealed at 450 K for several minutes, which has been shown to smooth the surface considerably without causing any intermixing.^{12,13} The Cu wedge was grown at $T=173$ K to avoid the formation of pyramidlike island.^{14,15} The second Ni layer was then grown at 293 K again after annealing the sample at about 450 K.

For the MSHG measurements light pulses from a Ti:sapphire laser (pulse width 80 fs, repetition rate 80 MHz) were focused onto the sample in the MBE chamber. The maximum fluence was about 1–2 mJ cm⁻². The SH light generated at the sample is detected by a photomultiplier. The fundamental light is blocked by a combination of a dielectric and colored glass filters. The total SH intensity is measured in the transverse geometry. For the measurements in the longitudinal and polar Kerr geometry a polarizer is placed in the outgoing beam path for polarization analysis of the SH light. The angle of incidence was about 38°. The direction of the externally applied magnetic field had an angle of about 33° with respect to the surface normal of the crystal. Therefore, the field has an in-plane component as well as a component perpendicular to the surface. The in-plane component of

magnetic field was parallel to the $\langle 110 \rangle$ azimuth. For all results on Ni films shown in this paper the wavelength of the incident light was 800 nm. The magneto-optical Kerr effect (MOKE) in the (linear) reflected light was measured in the longitudinal geometry as described in Ref. 16.

III. SIMPLE MODEL OF MSHG FROM COUPLED FM LAYERS

For the description of the SHG thought to be generated locally at interfaces a model based on the work of Sipe¹⁷ has been frequently applied in the past for ferromagnetic films and multilayers to separate the contribution from the individual interfaces.^{5,18–22} It is assumed in this model, that the SH light is generated only in an infinitesimal thin sheet at the interfaces of the individual metal films. In the dipole approximation the *second-order* polarization $\mathbf{P}^{(2,l)}(2\omega)$ at each interface is given by

$$P_i^{(l)}(2\omega) = \chi_{ijk}^{(l)} E_j^{(l)}(\omega) E_k^{(l)}(\omega), \quad (1)$$

where l numbers the interfaces. [The superscript (2) in $P_i^{(2,l)}(2\omega)$ and $\chi_{ijk}^{(2,l)}$ indicating the second order is suppressed in Eq. (1) and will be suppressed also in the following.] $\mathbf{E}^{(l)}(\omega)$ is the total electric-field amplitude at the fundamental frequency ω . The resulting SH light amplitude from the multilayer can be obtained by solving Maxwells equation for the 2ω component with the $\mathbf{P}^{(l)}(2\omega)$ as source term as described in detail in Ref. 19. The tensor elements of the *second-order* susceptibility $\chi^{(l)}$ can be classified as ‘‘nonmagnetic,’’ or as ‘‘magnetic’’ depending whether they change their sign upon magnetization reversal.²³

For a fixed geometry and polarization of the incident light the nonmagnetic and magnetic part of the susceptibility at one interface can be described by a single number each. We named these effective nonlinear susceptibilities as depicted in Fig. 1 for the present case of a Ni/Cu/Ni/Cu(001) multilayer. While the nonmagnetic tensor elements $\chi_{nm}^{(l)}$ are independent of the alignment of the magnetization direction in the two Ni films, $\chi_m^{(3)}$ and $\chi_m^{(4)}$ have the opposite sign in the antiferromagnetic (AF) alignment compared to the ferromagnetic (FM) alignment with the magnetization direction of the upper film unchanged.

For the total thickness of the multilayer much smaller than the wavelength of the light in the media the changes of phase and amplitude of the incident light within the multilayer can be neglected and the effective second order susceptibility of the individual layers can be simply summed up into a single magnetic and nonmagnetic susceptibility

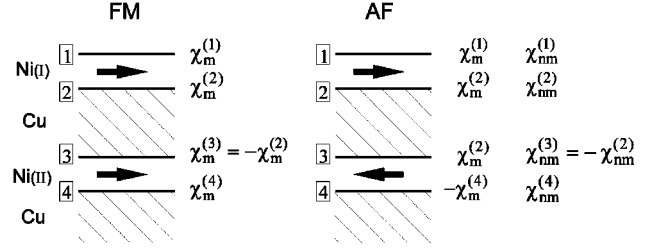
$$\chi_m^{\text{FM}} = \chi_m^{(1)} + \chi_m^{(4)}, \quad (2a)$$

$$\chi_m^{\text{AF}} = \chi_m^{(1)} - 2\chi_m^{(3)} - \chi_m^{(4)} \quad (2b)$$

for the FM and AF alignment of the magnetization in the Ni layers. The total nonmagnetic second-order susceptibility is given by $\chi_{nm} = \chi_{nm}^{(1)} + \chi_{nm}^{(4)}$ for both configurations. For the derivation we have assumed that

$$\chi_{nm}^{(3)} = -\chi_{nm}^{(2)} \quad \text{and} \quad \chi_m^{(3)} = -\chi_m^{(2)}. \quad (3)$$

(a) Ni/Cu/Ni/Cu(001)



(b) Cu/Ni/Cu(001)

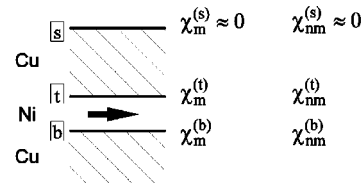


FIG. 1. Effective second-order susceptibilities $\chi_m^{(l)}$ and $\chi_{nm}^{(l)}$ from the different interfaces of a Ni/Cu/Ni/Cu(001) trilayer (a) and a Cu/Ni/Cu(001) bilayer (b). The arrow inside the Ni layers indicates the direction of the magnetization.

This assumption is motivated by the consideration, that in the case of infinite thick Ni films and a thin Cu layer the inversion symmetry of the total system is reestablished and therefore the total SHG from the structure must vanish, which requires the relation given in Eq. (3). Since in many cases the effective range about the interfaces, in which the second-order susceptibility is of significant size, is only a few (1– 2) ML thick, this consideration may even hold for quite thin Ni films. Then, with the same argument as above, $\chi_m^{(4)}$ should be equal to $-\chi_m^{(3)}$. (Alternatively, one may consider the case of an infinite thick Cu interlayer and thin Ni films, which would also yield $\chi_m^{(4)} = -\chi_m^{(3)}$.) It follows that there should be no net SHG from the bottom Ni film. However this is not what is experimentally observed. In Fig. 2 the hysteresis curves in the SH intensity measured (in the transverse geometry) on a 6 ML Ni/x-Cu/6 ML Ni/Cu(001) trilayer are shown for three thicknesses of the Cu interlayer, (a) 5 ML in the region of FM coupling of the two Ni films, and (b) and (c) for 10 ML and 24 ML, respectively, where AF coupling occurs. The details of the hysteresis curves will be discussed below. Here we want to emphasize, that FM and AF alignment of the magnetization in the top and bottom Ni layer can be clearly distinguished by the shape of the hysteresis curve. While for the FM coupling always a rectangular shaped hysteresis curve is observed as in Fig. 2(a) the SH intensity differs [either larger as in Fig. 2(b) for 10 ML or smaller as in Fig. 2(b) for 24 ML interlayer thickness] for the remanent state from the value at saturation. Clearly the bottom Ni layer must contribute to the magnetization induced SHG. [Because of very low interlayer coupling strength at 24 ML, the switching field in Fig. 2(c) amounts only to about 10 Oe compared to about 80 Oe for 10 ML.]

The reason for the different shape of the hysteresis curves

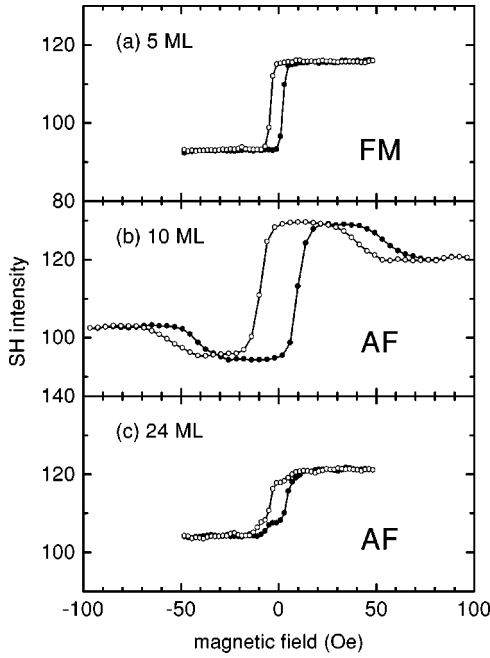


FIG. 2. Hysteresis curves of the SH intensity from 6 ML Ni/ x ML Cu/6 ML Ni/Cu(001) measured in the transverse geometry with p -polarized light at 220 K for three different thicknesses of the Cu interlayer: (a) 5 ML, (b) 10 ML, and (c) 24 ML. The solid and open circles indicate the measurements with increasing and decreasing field, respectively.

and the contribution of the bottom Ni film is that the electronic structure in thin Cu films is different from that of the bulk material. Additional thin-film states (quantum well states) appear in the Cu interlayer which may heavily influence the SHG. In case these QWS's are fully confined to the Cu interlayer, Eq. (3) still holds but interface (4) and (3) are now different, because only at interface (2) and (3) the QWS are present (if the QWS's are fully localized inside the Cu interlayer). Therefore the difference between $\chi_m^{(4)}$ and $-\chi_m^{(3)} = \chi_m^{(2)}$ describes the influence of the QWS's. Equation (2) can be rewritten as

$$\Delta\chi_m := \frac{1}{2}(\chi_m^{\text{FM}} - \chi_m^{\text{AF}}) = \chi_m^{(3)} + \chi_m^{(4)}. \quad (4)$$

Of course Eq. (4) is valid even without the assumption of Eq. (3). However, the nonzero difference $\Delta\chi_m$ is considered now as being caused by the fact, that at interface 3 QWS's from the Cu interlayer contribute while there are no such states at interface 4 on the substrate side of the trilayer. The possible different SHG caused by morphological differences between interfaces 3 and 4 caused by the differences of growth of Ni on Cu and Cu on Ni are less important and cannot explain the different shape of the hysteresis curves shown in Fig. 2 because this difference should be independent of the Cu interlayer thickness. The nonmagnetic tensor elements $\chi_{\text{nm}}^{(l)}$ are not affected by the direction of the magnetization and therefore $\chi_{\text{nm}}^{(l)}$ is identical for the FM and the AF alignment of the magnetization of the top and bottom layers.

For a Cu/Ni bilayer the contribution of QWS's to the magnetic second-order susceptibility is

$$\chi_m^{bl} = \chi_m^{(t)} + \chi_m^{(b)}. \quad (5)$$

with $\chi_m^{(t)}$ and $\chi_m^{(b)}$ defined as shown in Fig. 1(b).

There is no magnetic contribution $\chi_m^{(s)}$ from the Cu surface. The nonmagnetic contribution from the Cu surface, $\chi_{\text{nm}}^{(s)}$, is also very low at a wavelength of 800 nm of the incident light.^{6,24} Therefore all contributions from the surface of the Cu cover layer can be neglected and an equivalent equation to Eq. (5) is also true for χ_{nm} .

In case the QWS's are fully confined in the Cu cover layer or interlayer, respectively, then, as in the case of the trilayer, $\chi_m^{(t)}$ should be equal to $\chi_m^{(3)}$ and $\chi_m^{(b)} = \chi_m^{(4)}$.

In the experiments the SH intensity is measured, which for a fixed experimental condition is given by

$$I^\pm = |\chi_{\text{nm}} \pm \chi_m|^2 I_0^2, \quad (6)$$

where the I^+ and the I^- are the measured intensities for the magnetization of the sample in opposite directions and I_0 the intensity of the incident light. The average SH intensity is defined as

$$I_{\text{av}} := \frac{I^+ + I^-}{2} = |\chi_{\text{nm}}|^2 (1 + R^2) I_0^2, \quad (7)$$

with $R = |\chi_m / \chi_{\text{nm}}|$. It is useful to define an asymmetry

$$A := \frac{I^+ - I^-}{I^+ + I^-} = \frac{2R}{1 + R^2} \cos \phi, \quad (8)$$

with ϕ the phase angle between χ_m and χ_{nm} . For not too large $|\chi_m|$ the term proportional to R^2 can be neglected and A becomes proportional to the ratio of magnetic and nonmagnetic part of the second-order susceptibility. Similarly I_{av} is nearly proportional to $|\chi_{\text{nm}}|^2$.

In the present case of a (001) surface the SH light is entirely p polarized in the transverse geometry for p - or s -polarized incident light.¹ For the longitudinal geometry the polarization of the SH light generated by χ_{nm} and χ_m have different polarization p and s , respectively. Therefore the asymmetry $A(\alpha)$ measured as a function of the analyzer angle α placed in the outgoing beam path, is given by

$$A(\alpha) = \frac{2R \tan \alpha}{1 + R^2 \tan^2 \alpha} \cos \phi, \quad (9)$$

where $\alpha=0$ corresponds to p -polarized light.

IV. RESULTS

A. Quantum size effects in Cu/Ni/Cu(001) sandwiches

Figure 3 shows the p -polarized SH intensity from sandwich structures of Cu/4.3 ML Ni/Cu(001) (c) in comparison with similar measurements on Cu/3 ML Fe/Cu(001) (a), and Cu/10 ML Co/Cu(001) (b), all measured with p -polarized

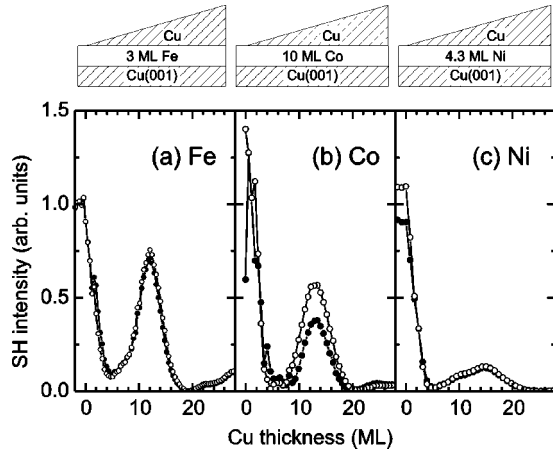


FIG. 3. p -polarized SH intensity as a function of the Cu cover layer from (a) Cu/3 ML Fe/Cu(001), (b) Cu/10 ML Co/Cu(001), and (c) Cu/4.3 ML Ni/Cu(001) measured with p -polarized incident light. In (a) the magnetization of the Fe film was (mainly) perpendicular to the surface plane while in (b) and (c) the magnetization was in the surface plane and perpendicular to the optical plane (transverse geometry). The solid and open symbols indicate the SH intensity for the magnetization in opposite directions.

incident light. For the 3 ML Fe is the easy axis of magnetization (mainly) perpendicular to the sample surface and therefore no (large) difference in the SH intensity for the magnetization in opposite directions (open and solid symbols in Fig. 3) is observed in the entirely p -polarized SH intensity. For the case of Co and Ni the magnetization of the ferromagnetic film is in the surface plane (transverse geometry) and therefore an asymmetry in the p -polarized SH intensity is observed. Nevertheless, for most Cu cover layer thicknesses it is small enough, so that the average SH intensity can be considered as being proportional to $|\chi_{nm}|^2$ except near the minima of the curves. The wavelength for the three different measurements in Fig. 3 are slightly different, 770 nm, 790 nm, and 800 nm for the Fe, Co, and Ni sandwich. (For the present discussion this small wavelength difference is not important. A detailed discussion of the wavelength dependence can be found in Ref. 8.)

Let us focus on the average SH intensity first. As has been discussed in Refs. 25 and 8, the observation, that the SH intensity initially drops with increasing Cu cover layer thickness for all three cases, can be explained by the fact, that upon Cu coverage of the transition metal film, the electronic structure at the top and bottom buried interfaces become more similar. In the absence of any thin-film states in the Cu cover layer the SH light generated at these two interfaces exactly cancel each other because of the “restored” inversion symmetry if the thickness of the transition metal film can be neglected against the optical wavelength in the metal. However, thin-film states which are localized at the Cu cover layer (quantum well states) strongly affect the electronic properties of the top Cu/transition metal interface and cause the oscillatorylike intensity changes with increasing Cu thickness.²⁵ We emphasize that the maxima at 12–15 ML are caused by the influence of the QWS’s on the nonmagnetic part of the second-order susceptibility, χ_{nm} , since they occur

in the average SH intensity I_{av} and χ_m is small at that Cu thickness compared to χ_{nm} . Although the detailed shape of the SH intensity vs Cu thickness curve depends strongly on the wavelength of the incident light and to some extent on the preparation conditions of the ferromagnetic film and the Cu cover layer we made the general observation, that in the case of the Ni sandwich the SH intensity of the maximum at about 12–15 ML never reached such large values observed for Co and especially for Fe sandwiches. Therefore, we suppose that the QWS influence on χ_{nm} is weakest in the case of a Cu/Ni bilayer.

The understanding of the magnetic signal vs Cu cover layer thickness especially in the case of an Fe or Co sandwich is complicated by the fact that in the region near 5 ML and at large Cu thickness the contribution to the SHG from χ_m becomes comparable or even larger than that from χ_{nm} and the exact relations, Eqs. (7) and (8) have to be used. Only by additional measurements in a geometry, where χ_m and χ_{nm} lead to SH light with different polarization this separation including the complex phase ϕ between χ_m and χ_{nm} can be made unambiguously. For Cu/Co/Cu(001) wedges it has been found, that in the longitudinal geometry χ_m is only weakly affected by the QWS’s and only at very thin Cu cover layer of 1 or 2 ML strong changes in $|\chi_m|$ have been observed.^{8,25} The case of Cu/Ni/Cu(001) sandwiches will be discussed below. Here we simply state that the SH asymmetry vs Cu cover thickness in all these sandwich structures is *not* proportional to $|\chi_m|$ nor even to the magnetization of the ferromagnetic film.

B. Exchange coupled Ni/Cu/Ni/Cu(001) layers

1. Transverse Kerr geometry

Figure 4 shows as a hysteresis curve measured by MOKE [Fig. 4(a)] and by MSHG (b) from a 6 ML Ni/ x ML Cu/6 ML Ni/Cu(001) trilayer structures at a Cu thickness of 10 ML, where the two Ni films couple antiferromagnetically.²⁶ It is known, that the magnetization and the Curie temperature of thin Ni films is reduced when covered with Cu.^{27,28} At 220 K we observed for a 6 ML Ni film on Cu(001) a decrease of the MOKE rotation by almost a factor of 3 when covered with a Cu layer. Therefore, it is reasonable to assume that the magnetization of the lower film is smaller than that of the top Ni film. In Fig. 4 the direction of the magnetization of the top and bottom Ni film is indicated by long and short arrows. At large negative external field, the magnetization of the top and bottom Ni film are aligned parallel to the external field (left). Starting at saturation at $H = 150$ Oe, first the lower Ni film (having the lower magnetization) reverses its magnetization direction at about -80 Oe with increasing external field. At about $+6$ Oe both, the top and the bottom Ni film inverse their magnetization simultaneously before at large positive external fields the lower Ni film reverses its magnetization again and the magnetization of both films is aligned in the direction of the external field. Although not strictly true the total linear MOKE signal from the individual Ni layers can be thought as the sum of the two individual contribution from the top and the bottom layer since the total multilayer is much thinner than the penetration depth of the

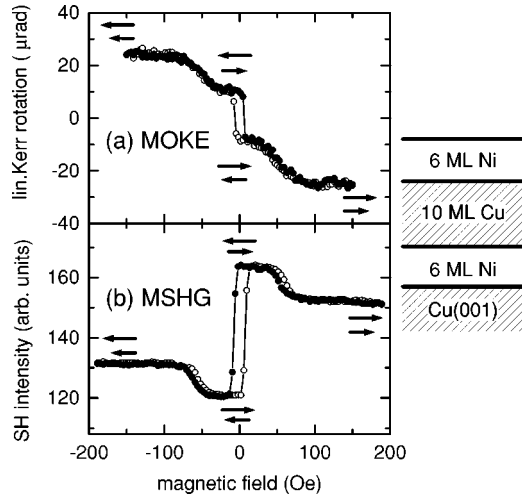


FIG. 4. Kerr hysteresis loop from a 6 ML Ni/10 ML Cu/6 ML Ni/Cu(001) multilayer structure in the antiferromagnetic coupling range (a) in the linear reflected light and (b) in the SH light measured at a sample temperature of $T_s = 220$ K. The arrows represent the magnetization direction of the upper (long arrow) and lower (short arrow) Ni film. The solid (open) symbols represent the measurements with increasing (decreasing) field. Note, despite the same thickness of both films the magnetic moment of the lower film is reduced.

light.²⁹ Therefore, the parallel alignment of magnetization of the upper and lower Ni film gives the larger MOKE signal (approximately proportional to the sum of the magnetic moments of top and bottom film) while at antiparallel alignment the total Kerr signal is reduced (approximately proportional to the difference of the magnetic moment of upper and lower film).

This is *not* the case for the magneto-optical effect in the SHG as can be seen in Fig. 4(b). The maximum change of SH light intensity is observed at remanence. The SH light intensity remains always much larger than its changes. (Note the zero suppression in Fig. 4(b). This allows us to assume a linear dependence of χ_m on the SH asymmetry. However, the individual magnetic contributions from the different interfaces, $\chi_m^{(l)}$, are complex numbers and therefore the difference $\Delta\chi_m$ in Eq. (4) can lead to an increase or decrease of the ratio R , depending whether this difference leads to an increase or decrease of the projection of the total magnetic susceptibility χ_m onto χ_{nm} . The effective phase factor ϕ in Eq. (8) is important and this factor may change with, for example, the wavelength of the incident light, the incident angle, etc. Especially it may change with the thickness of the Cu interlayer. This has already been shown in Figs. 2(b) and 2(c). While for a Cu interlayer thickness of about 10 ML the QWS contribution $\Delta\chi_m$ leads to an enhancement of the SH Kerr signal in the AF aligned state of the magnetization with respect to the FM aligned state, for about 24 ML, where also AF coupling occurs, $\Delta\chi_m$ causes a reduction of the Kerr signal. Note, that within the model described in Sec. III the fact that the SH asymmetry is different for FM and AF alignment of the layers is a direct evidence of the influence of the QWS's on χ_m . In case the electronic structure at interfaces 3

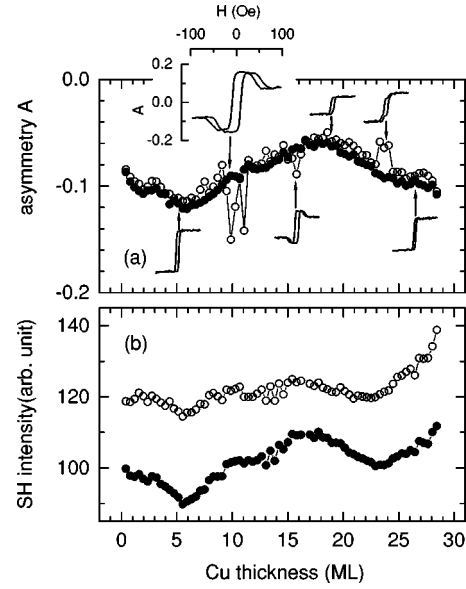


FIG. 5. SH asymmetry (a) and SH intensity (b) as a function of the Cu spacer layer from 6 ML Ni/ x ML Cu/6 ML Ni/Cu(001) measured in the transverse geometry with p -polarized light at 220 K. The solid and open circles in (a) indicate the asymmetry with (solid) and without (open) external field of about 190 Oe. The open and solid squares in (b) represent the SH intensity with applied external field in opposite directions.

and 4 are identical, thus $\chi_m^{(3)} = \chi_m^{(4)}$, the different coupling should be invisible in the SH asymmetry according to Eq. (4).

In Fig. 5 the SH intensities with an applied external transverse magnetic field of about 190 Oe, I^+ (solid circles) and I^- (open circles) (b) from a 6 ML Ni/ x ML Cu/6 ML Ni trilayer are plotted vs the Cu interlayer thickness. In Fig. 5(a) the corresponding SH asymmetry is plotted as solid symbols. In addition the SH asymmetry in the remanent states is shown as open symbols. Due to the steep slope of the Cu wedge of about 4 ML/mm not all regions of AF coupling are resolved. However, as can be seen from the SHG hysteresis loops plotted as insets in Fig. 5 AF coupling occurs at Cu thickness of about 10 ML, 16 ML, and 24 ML while at 5 ML, 19 ML, and 26 ML the shape of the hysteresis curve is consistent with FM coupling.

Without the presence of the QWS's in the Cu interlayer, a monotonous and nearly constant SH intensity as well as SH asymmetry would be expected from the model in Sec. III. This is not the case. Both, SH intensity and asymmetry show a long periodic oscillation of about 20–25 ML in Fig. 5. The changes in the average SH intensity I_{av} are relatively small but the variation in the asymmetry for the FM aligned layers amount to rather large 30%. We will postpone the discussion of this observation to Sec. V and we continue to assume the (approximate) validity of the model in Sec. III for the following.

As mentioned above, the observed difference in A for FM and AF alignment is caused by the QWS contribution to the Ni/Cu interface. The phase of the difference $\Delta\chi_m = \chi_m^{(3)} + \chi_m^{(4)}$ oscillates with the thickness of the Cu interlayer as

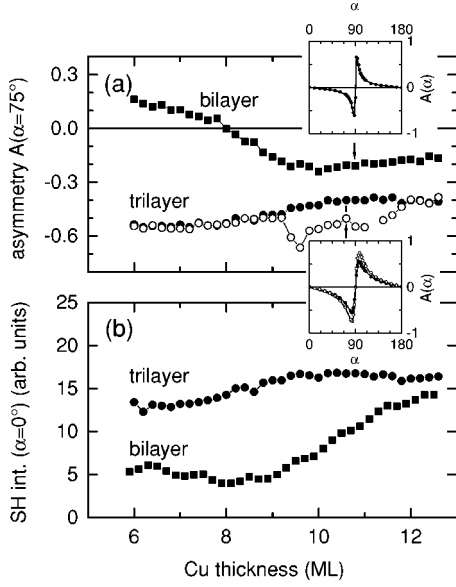


FIG. 6. MSHG from a trilayer (circles) and bilayer (squares) measured in the longitudinal geometry with s -polarized incident light. (a) asymmetry at $\alpha=75^\circ$, (b) p -polarized SH intensity ($\alpha=0^\circ$) as a function of the Cu spacer layer from 6.1 ML Ni/ x ML Cu/6.3 ML Ni/Cu(001) measured at 120 K. The insets show the $A(\alpha)$ curves for the Cu/Ni bilayer at 10.8 ML and the Ni/Cu/Ni trilayer at 10.6 ML Cu thickness. The solid lines are fit curves using Eq. (9). The solid and open circles in (a) indicate always the asymmetry with (solid) and without (open) external field of about 190 Oe.

shown in Figs. 2 and 5. In this transverse geometry only the projection of $\Delta\chi_m$ onto χ_{nm} can be observed but we find that for $d=10$ ML the QWS contribution is added to the “non-QWS” asymmetry while for $d=24$ ML it is subtracted. In the longitudinal geometry this phase difference can be extracted from the experimental data as will be shown in the next subsection.

2. Longitudinal Kerr geometry

Figure 6 shows similar SH measurements from 6.1 ML Ni/ x ML Cu/6.3 ML Ni/Cu(001) as those shown in Fig. 5 but for the longitudinal geometry with s -polarized light. (We used here s -polarized light, because the SH asymmetry for p -polarized incident light was very small.) The asymmetry is shown in Fig. 6(a) for an analyzer angle set to $\alpha=75^\circ$ from p polarization, while in Fig. 6(b) the p -polarized intensity ($\alpha=0^\circ$) is plotted. Although arbitrary units, the SH intensities can be compared within an accuracy of about 10–20% to those of Fig. 4 which are about a factor of 7 larger. The variations of the SH intensity with the Cu interlayer is somewhat larger [$\pm 10\%$ in the displayed thickness range than for p -polarized light ($\pm 5\%$)] but the thickness dependence can be considered as weak compared to that of the bilayer shown in Fig. 6(b) as squares. Looking at the SH asymmetries in Fig. 6(a) a similar behavior is found: a reasonably constant asymmetry for the trilayer in the FM state (solid circles) while the asymmetry for the bilayer (solid squares) even change sign at 8 ML. The region of AF coupling in the

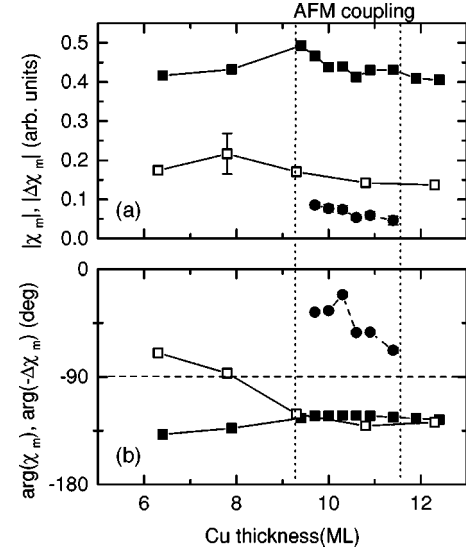


FIG. 7. The module (a) and phase (b) of χ_m and $\Delta\chi_m$ as a function of the Cu interlayer thickness derived from MSHG measurements from a 6.1 ML Ni/ x ML Cu/6.3 ML Ni/Cu(001) multilayer structure in the longitudinal geometry with s -polarized light at 120 K. The solid squares represent $\chi_m^{(1)} + \chi_m^{(4)}$ and the solid circles $\Delta\chi_m = \chi_m^{(3)} + \chi_m^{(4)}$. For comparison $\chi_m^{(bl)} = \chi_m^{(r)} + \chi_m^{(b)}$ derived from a x ML Cu/6.3 ML Ni/Cu(001) bilayer is included as open circles. (With the exception of the one data point near 8 ML the statistical errors are less than the symbol size.)

trilayer between about 9.5 and 11.5 ML can be identified by the difference of the asymmetry measured in remanence (open circles) and saturation.

In this longitudinal geometry the module $|\chi_m|$ and the phase difference ϕ between χ_m and χ_{nm} can be determined by measuring the SH asymmetry as a function of the polarizer angle α as shown in the insets in Fig. 6(a) for the Cu/Ni bilayer at 10.8 ML and for the Ni/Cu/Ni trilayer at 10.6 ML. (An s -polarized coherent SH background of less than 10% of the light amplitude has been subtracted from the data, resulting from slight misalignment of the optical plane and the incomplete polarization of the incident fundamental light.) The fit of the measured $A(\alpha)$ values to Eq. (9) yield R and ϕ for the FM (saturation) and AF alignment (remanence in AF coupling regions), from which the quantities $|\chi_m^{(1)} + \chi_m^{(4)}|$ and $|\chi_m^{(3)} + \chi_m^{(4)}|$ can be calculated using $I(\alpha=0) = |\chi_{nm}|^2 I_0^2$. These are plotted in Fig. 7(a) as solid squares and solid circles. The corresponding phases with respect to χ_{nm} are shown in Fig. 7(b). Module and phase of $\chi_m^{(bl)}$ obtained from measurements of a Cu/6.3 ML Ni/Cu(001) bilayer are included in Fig. 7 as open circles. Except for the data point at 8 ML for the bilayer all statistical errors are within the symbol size. We note that both the module and the phase for $\chi_m^{(1)} + \chi_m^{(4)}$, which is the contribution expected from a single Ni film, does not change much, as expected from the model. The QWS induced part is only measurable in the AF coupling region. Its relative strength is quite low and, other than expected from the model, definitely lower than $\chi_m^{(bl)}$.

$|\chi_m^{(r)} + \chi_m^{(b)}|$ of the bilayer is almost constant. It is only the phase which shows a large variation and passes 90° at 8 ML.

Note, only the relative phase between χ_m and χ_{nm} is determined. Therefore the observed change can be caused by an absolute phase change of χ_{nm} as well, and very likely it is, as will be discussed below.

V. DISCUSSION

Despite the efforts made in the theoretical description of MSHG from metal surfaces and interfaces up to now there is no quantitative theoretical description which can be compared to experimental values.^{9,23,30–35} While for simple metals like Al, Liebsch developed a theory, which properly accounts for the dynamic screening effects in the presence of the electric field of the light^{36,37} is in semiquantitative agreement with experiments,^{38,39} this theory has not yet been extended to 3d-metals. Therefore, currently one is restricted to simple phenomenological models like that presented in Sec. III to describe the experimental data. A more elaborated model has been described in Ref. 19, which includes the local-field effects of the fundamental and SH light using bulk optical constants. This model is still based on the dipole approximation and localized second-order susceptibilities at the interfaces, but is capable to describe the thickness dependence of the SH intensity as a function of the layer thickness for thick films, where quantum size effects can be ignored. However, in the present case of ultrathin films this more complicated model would predict only a monotonous increase or decrease of the SH intensity and/or asymmetry with the layer thickness. It is unable to describe the fast oscillatorylike behavior of the SH intensity as a function of the Cu layer in the bilayer systems and does not lead to a better description of the experimental results than the simple model of Sec. III.

It has been shown, for example, in Cu(001) at a photon energy of the fundamental light below the *d*-band threshold, that nonlocal quadrupolelike contribution can become comparable to the local dipole contribution.²⁴ Especially for the *p*-polarized SH response from interfaces of *d*-metal films like Fe, Co, and Ni, however, it was found that the dipole contribution is much higher than that from Cu at the same photon energy.^{6,8,40,41} Therefore, the nonlocal contributions are much less important for these transition-metal films.⁸

In metallic sandwich structures of 3d-metal films covered by noble metals like Cu and Au a strong influence of the SH intensity on the noble metal cover layer has been observed. This has been explained within the dipole approximation by a resonance phenomenon between thin-film states of the noble metal and states derived from the 3d-metal states.^{8–10} A similar interpretation was used in Ref. 11 for the observed oscillations of the SHG from Ag/Si(111) while the oscillations observed in the SHG from Rb/Ag(110) (Ref. 42) were interpreted by dynamic screening (induced Friedel oscillations). In the latter case almost all SH is generated in the Rb layer, since the SH intensity from the Ag(110) increases by more than three orders of magnitude when covered with Rb. However, the observed oscillations in the other above-mentioned cases cannot be described by this effect, since the oscillations are observed not only for *p*-polarized light as in Ref. 42 but for *s*-polarized light as well.^{7,8,19}

A necessary prerequisite for the QWS's to contribute to the SHG is a certain amount of hybridization with states of the Ni film to break the symmetry. The symmetric (with respect to the inversion at the center of the film) as well as the antisymmetric QWS's wave functions of the Cu film do not cause any SHG from the isolated film. Since the very low SH intensity of a bare Cu surface is expected from the Cu/Ni bilayer, if the QWS do not affect the SHG, this may indicate a weaker hybridization of the 4s QWS band in the Cu with the 3d bands of the Ni film. However, the energetic position of the 3d states of the ferromagnetic film at the interface may also affect the SHG.⁸ Because the QWS oscillations do occur mainly in χ_{nm} , magnetic effects like the change of the magnetic spin or orbital moment at the interface are less important.⁴³

The observation of the Cu thickness dependence in the Ni/Cu/Ni trilayer in the FM aligned state is not expected from a model of local SHG generation as presented in Sec. III. However, this does not necessarily imply, that the dipole approximation is not valid. As discussed, for example, in Ref. 44 the QWS's near the Fermi energy are only weakly confined to the Cu interlayer. They rather extend through the whole layer stack. Therefore, not only the interfaces in the neighborhood of the Cu interlayer, but the bottom interface (4) as well as the surface (1) are affected and the expressions $\chi_m^{(1)} + \chi_m^{(4)}$ and $\chi_{nm}^{(1)} + \chi_{nm}^{(4)}$ become a (weak) function of the Cu interlayer, which may cause the observed oscillatorylike change of the SH intensity and asymmetry in the FM aligned state of the trilayer. Because the *d*-band electrons of the Ni are much more localized, the SHG may still be strongly peaked at the interfaces.

Therefore, the presence of the oscillations in the SH asymmetry in the FM aligned state imply that the difference $\Delta\chi_m$ is not exactly the difference in the second-order susceptibility at the Ni/Cu film interface (2) and the Ni/Cu bulk interface (4) as written in Eq. (4) but, because the interface (4) is affected by the QWS's as well, $\Delta\chi_m$ describes the difference between the Ni/Cu film interface (2) and the Ni/Cu interface (4), which is *modified* by the thin-film states of the Ni/Cu/Ni trilayer. (The modification of $\chi_m^{(1)}$ by the QWS's of the trilayer cancels out.)

The analysis of the MSHG measurements in the longitudinal geometry allow a separation of the magnetic tensor elements, which removes all thickness dependence of χ_{nm} . There the ‘‘Ni film’’ component $\chi_m^{(1)} + \chi_m^{(4)}$ shows indeed a rather constant value over the investigated thickness range from 6 to 13 ML, which is not too surprising, since most of the net SH light is generated from the top film. The analysis of the bilayer shows, similar to what was found for the Cu/Co bilayer,⁸ only a weak thickness dependence of the magnetic components. The comparison with $\Delta\chi_m$ of the trilayer, reveals clearly the quantitative discrepancy to the model, now pointed down to the magnetization induced part. The neglected depth dependence of the electric fields of the incident fundamental and outgoing SH light amounts only to approximately 13% reduction for the trilayer compared to the bilayer due to the reflection/adsorption on the top Ni film. We note, that the different behavior of the phase of $\Delta\chi_m$ and

χ_m^{bl} is not unexpected, since the corresponding nonmagnetic effective tensor elements are different.

Despite its failure of a quantitative description the simple model still gives the qualitatively correct answer: The fact, that AF coupling can be observed in the SHG hysteresis curves from ultrathin Ni layers coupled through a Cu interlayer is caused by the QWS's. The strong deviations found in the present case might be caused to a major part by the fact, that the QWS's extend over the entire layer stack—at least for a substantial energy range. In a system, where the QWS's are strongly confined to the interlayer a better agreement with the model is expected.

VI. CONCLUSION

In this paper we have shown that interlayer coupling in ultrathin Ni/Cu/Ni trilayers on Cu(001) can be observed by MSHG despite the fact that MSHG is interface sensitive and

in no way proportional to the net magnetization of the trilayer. The observed magnetic contrast change in the SH light intensity is caused by the presence of quantum well states in the Cu spacer layer, which lifts the complete destructive interference of the Ni/Cu and Cu/Ni interface, which otherwise would occur. Although the simple model of local SH generation at the interfaces does not give quantitatively correct results in ultrathin multilayers, it still can be used in these cases for a qualitative description of MSHG.

ACKNOWLEDGMENTS

One of the authors, Y. Z. Wu, acknowledges the MPI Halle for financial support during his stay. He also acknowledges the partial support from the National Natural Science Foundation (Grant Nos. 19625410 and 19734002). This work was supported in part by the EC through Grant No. ERB-EMRX-CT96-0015 (TMR NOMOKE).

*Author to whom correspondence should be addressed. Electronic address: vollme@mpi-halle.mpg.de

¹*Nonlinear Optics at Metallic Interfaces*, edited by K.-H. Bennemann (Oxford University Press, Oxford, 1998).

²R. Vollmer, M. Straub, and J. Kirschner, *J. Magn. Soc. Jpn.* **20**, 29 (1996).

³R. Vollmer, M. Straub, and J. Kirschner, *Surf. Sci.* **352**, 937 (1996).

⁴B. Koopmans, M.G. Koerkamp, Theo Rasing, and H. van den Berg, *Phys. Rev. Lett.* **74**, 3692 (1995).

⁵H.A. Wierenga, W. de Jong, M.W. Prins, Th. Rasing, R. Vollmer, A. Kirilyuk, H. Schwabe, and J. Kirschner, *Phys. Rev. Lett.* **74**, 1462 (1995).

⁶R. Vollmer, A. Kirilyuk, H. Schwabe, J. Kirschner, H.A. Wierenga, W. de Jong, and Th. Rasing, *J. Magn. Mater.* **148**, 295 (1995).

⁷A. Kirilyuk, Th. Rasing, R. Mégy, and P. Beauvillain, *Phys. Rev. Lett.* **77**, 4608 (1996).

⁸R. Vollmer, in *Nonlinear Optics at Metallic Interfaces*, edited by K.-H. Bennemann (Oxford University Press, Oxford, 1998), Chap. 2, pp. 42–131.

⁹T. Luce, W. Hübner, and K.H. Bennemann, *Phys. Rev. Lett.* **77**, 2810 (1996).

¹⁰T.A. Luce, W. Hübner, A. Kirilyuk, Th. Rasing, and K.H. Bennemann, *Phys. Rev. B* **57**, 7377 (1998).

¹¹Thomas Garm Pedersen, K. Pedersen, and Thomas Brun Kristensen, *Phys. Rev. B* **60**, R13 997 (1999).

¹²J. Shen, J. Giergiel, and J. Kirschner, *Phys. Rev. B* **52**, 8454 (1995).

¹³J. Shen, M.-T. Lin, J. Giergiel, C. Schmidhals, M. Zharnikov, C.M. Schneider, and J. Kirschner, *J. Magn. Mater.* **156**, 104 (1996).

¹⁴C. Würsch, C. Stamm, S. Egger, D. Pescia, W. Baltensperger, and J.S. Helman, *Nature (London)* **389**, 937 (1997).

¹⁵H.-J. Ernst, F. Fabre, and J. Lapujoulade, *Phys. Rev. B* **46**, 1929 (1992).

¹⁶Y. Z. Wu, R. Vollmer, H. Regensburger, and J. Kirschner, *Phys. Rev. B* **62**, 5810 (2000).

¹⁷J.E. Sipe, *J. Opt. Soc. Am. B* **4**, 481 (1987).

¹⁸H.A. Wierenga, M.W.J. Prins, D.L. Abraham, and Th. Rasing, *Phys. Rev. B* **50**, 1282 (1994).

¹⁹H.A. Wierenga, M.W.J. Prins, and Th. Rasing, *Physica B* **204**, 281 (1995).

²⁰H.A. Wierenga, W. de Jong, M.W.J. Prins, Th. Rasing, R. Vollmer, A. Kirilyuk, H. Schwabe, and J. Kirschner, *Surf. Sci.* **331-333**, 1294 (1995).

²¹Q.Y. Jin, H. Regensburger, R. Vollmer, and J. Kirschner, *Phys. Rev. Lett.* **80**, 4056 (1998).

²²A. Kirilyuk, Th. Rasing, M.A.M. Haast, and J.C. Lodder, *Appl. Phys. Lett.* **72**, 2331 (1998).

²³R.-P. Pan, H.D. Wei, and Y.R. Shen, *Phys. Rev. B* **39**, 1229 (1989).

²⁴R. Vollmer, M. Straub, and J. Kirschner, *Surf. Sci.* **352-354**, 684 (1996).

²⁵R. Vollmer, Q.Y. Jin, H. Regensburger, and J. Kirschner, *J. Magn. Mater.* **198-199**, 611 (1999).

²⁶The top Ni film was in the “as grown” state and not annealed for the data shown in Figs. 2–5. Recently we showed in Ref. 16 that the roughness of the surface of the topmost Ni film strongly influences the interlayer coupling. Therefore antiferromagnetic coupling is observed at 10 ML while in the annealed trilayer structure in Ref. 16 the Ni films couple ferromagnetically at 10 ML.

²⁷P. Srivastava, F. Wilhelm, A. Ney, M. Farle, H. Wende, N. Haack, G. Ceballos, and K. Baberschke, *Phys. Rev. B* **58**, 5701 (1998).

²⁸S. van Dijken, R. Vollmer, B. Poelsema, and J. Kirschner, *J. Magn. Mater.* **210**, 316 (2000).

²⁹Z.Q. Qiu, J. Pearson, and S.D. Bader, *Phys. Rev. B* **46**, 8659 (1992).

³⁰W. Hübner and K.-H. Bennemann, *Phys. Rev. B* **40**, 5973 (1989).

³¹W. Hübner, *Phys. Rev. B* **42**, 11 553 (1990).

³²U. Pustogowa, W. Hübner, and K.H. Bennemann, *Phys. Rev. B* **48**, 8607 (1993).

³³P. van Geldern, S. Crampin, Th. Rasing, and J.E. Inglesfield, *Phys. Rev. B* **54**, R2343 (1996).

³⁴J.P. Dewitz, J. Chen, and W. Hübner, *Phys. Rev. B* **58**, 5093 (1998).

- ³⁵V.L. Brundy, W.L. Mochán, A.V. Petukhov, Th. Rasing, and B.S. Mendoza, *Phys. Status Solidi A* **170**, 227 (1998).
- ³⁶A. Liebsch, *Phys. Rev. Lett.* **61**, 1233 (1988).
- ³⁷A. Liebsch and W.L. Schaich, *Phys. Rev. B* **40**, 5401 (1989).
- ³⁸R. Murphy, M. Yeganeh, K.J. Song, and E.W. Plummer, *Phys. Rev. Lett.* **63**, 318 (1989).
- ³⁹S. Janz, K. Pedersen, and H.M. van Driel, *Phys. Rev. B* **44**, 3943 (1991).
- ⁴⁰V. Jähnke, U. Conrad, J. Güdde, and E. Matthias, *Appl. Phys. B: Lasers Opt.* **68**, 485 (1999).
- ⁴¹M. Straub, R. Vollmer, and J. Kirschner, *Phys. Rev. Lett.* **77**, 743 (1996).
- ⁴²K.J. Song, D. Heskett, H.L. Dai, A. Liebsch, and E.W. Plummer, *Phys. Rev. Lett.* **61**, 1380 (1988).
- ⁴³O. Hjortstam, J. Trygg, J.M. Wills, B. Johansson, and O. Eriksson, *Phys. Rev. B* **53**, 9204 (1996).
- ⁴⁴K. Wildberger, R. Zeller, P.H. Dederichs, J. Kudrnovský, and P. Weinberger, *Phys. Rev. B* **58**, 13 721 (1998).